

Progress Report of the HypHI Phase 0 experiment (S319) at GSI:

Hypernuclear spectroscopy of ${}^3_{\Lambda}\text{H}$, ${}^4_{\Lambda}\text{H}$ and ${}^5_{\Lambda}\text{He}$
with a ${}^6\text{Li}$ beam at 2 A GeV on a ${}^{12}\text{C}$ target

March 18th, 2007

The HypHI collaboration

Beijing, China, Department of Technical Physics, Peking University

H. Lu

Copenhagen, Denmark, The Niels Bohr Institute

G. Hagemann, B. Herskind, G. Sletten

Darmstadt, Germany, Experimentelektronik, GSI

J. Adamczewski, H.G. Essel, J. Hoffmann, N. Kurz

Darmstadt, Germany, Kernphysik II, GSI

T. Aumann, H. Geissel, J. Gerl, M. Kavatsyuk, O. Lepyoshkina, Y. Litvinov,
G. Münzenberg, C. Rappold, T.R. Saito, H. Schaffner, H. Simon, H. Weick, M. Winkler

Darmstadt, Germany, Kernphysik III, GSI

A. Le Fèvre, U. Lynen, W.F.J. Müller, H. Orth, C. Schwarz, C. Sfienti, W. Trautmann

Dubna, Russia, Frank Laboratory of Neutron Physics, JINR

T.Yu. Tretyakova

Kyoto, Kyoto University, RIKEN

K. Tanida

Mainz, Germany, Institut für Kernphysik, Johannes-Gutenberg Universität Mainz

P. Achenbach, C. Ayerbe, S. Minami, J. Pochodzalla, A. Sanchez-Lorente

Moscow, Russia, Institute of Nuclear Physics, Moscow State University

D.E. Lansky

Nara, Japan, Physics Department, Nara Women's University

E. Hiyama

Neyagawa, Japan, Division of Electronics and Applied Physics, Osaka

Electro-Communication University

T. Fukuda, Y. Mizoi, T. Motoba

Noda, Japan, Faculty of Science and Technology, Tokyo University of Science

M. Kurosawa, K. Nakai

Sendai, Japan, Physics Department, Tohoku University
O. Hashimoto, T. Koike, T. Nakamura, H. Tamura, A. Tsukada, M. Ukai

Tokyo, Japan, Faculty of Science, Tokyo University
H. Fujioka, T. Maruta, D. Nakajima

Toyonaka, Japan, Graduate School of Science, Osaka University
S. Ajimura, T. Kishimoto, A. Sakaguchi

Tsukuba, Japan, Institute of Particle and Nuclear Studies, KEK
J. Chiba, T. Nagae, H. Noumi, Y. Sato, M. Sekimoto, H. Takahashi, T. Takahashi,
A. Toyoda

Vancouver, Canada, TRIUMF
I. Tanihata

Wako, Japan, Advanced Meson Science Laboratory, RIKEN
S. Okada, H. Outa

Warsaw, Poland, Soltan Institute for Nuclear Studies
B. Zwieglinski

Spokesperson : T.R. Saito, GSI. t.saito@gsi.de

Abstract

The HypHI collaboration is recently preparing for the Phase 0 experiment in order to demonstrate the feasibility of precise hypernuclear spectroscopy with heavy ion beams. In the Phase 0 experiment, light hypernuclei such as ${}^3_{\Lambda}\text{H}$, ${}^4_{\Lambda}\text{H}$ and ${}^5_{\Lambda}\text{He}$ will be investigated with a primary beam of ${}^6\text{Li}$ at 2 A GeV impinged on a ${}^{12}\text{C}$ target. Design studies for the experimental setup have been completed with Monte Carlo simulations, and a proposal of the Phase 0 experiment was presented to G-PAC 33 in 2006 in order to ask 45 shifts for the Phase 0 experiment. The HypHI collaboration was granted seven night shifts by G-PAC 33 for testing detectors and trigger systems. In the letter from G-PAC 33, issues on the trigger system and the event generator of Monte Carlo simulations were discussed, and we would like to answer to the questions by G-PAC 33 in this progress report. In this report, progresses on the development of scintillating fiber detectors, the tracking trigger system, the TOF wall for positively charged particles and drift chambers will be discussed. We spent granted three night shifts in March 2007 to test prototypes of scintillating fiber detectors and the tracking trigger with a primary beam of ${}^{12}\text{C}$ at 2 A GeV and a cocktail beam with π^+ , proton, deuteron, triton and ${}^3\text{He}$ at 3.3 Tm. The results of the test experiment will be discussed in the report, which demonstrates the feasibility of tracking by proposed scintillating fiber detectors and of the tracking trigger. The report also discusses on the transport calculations for an event generator of Monte Carlo simulations, including a comparison between the UrQMD and IQMD calculations. In addition to those transport calculations, preliminary results of another transport calculation, GiBUU, will be discussed. By these investigations, the request to G-PAC 34 has not been changed from the one to G-PAC 33, therefore, we would like to request 45 shifts for the Phase 0 experiment.

Contents

1	Introduction to the HypHI Phase 0 experiment	5
2	Progress of developments for detectors and trigger systems	7
2.1	Scintillating fiber detectors and tracking trigger	7
2.1.1	Tests with cosmic-rays, radiation sources and lasers	8
2.1.2	Test with ^{12}C beams at 2 A GeV and cocktail beams at 3.3 Tm . . .	10
2.1.3	Final design of scintillating fiber detectors	15
2.1.4	Development and production of new VME logic modules for the tracking trigger	16
2.2	TOF+: a TOF wall for positively charged particles	17
2.3	Drift chambers	18
3	Progress on transport calculations as event generator of Monte Carlo simulations	19
3.1	Comparison between UrQMD and IQMD	20
3.2	New calculations by the Giessen Boltzmann-Uehling-Uhlenbeck project (GiBUU)	23
4	Conclusion and request	26

1 Introduction to the HypHI Phase 0 experiment

Comprehensive understanding of the universe requires to study baryon-baryon interactions under flavored-SU(3) with up-, down- and strange-quarks. Baryon-baryon interactions involving a hyperon which is a baryon with at least one strange quark have been mainly studied via hypernuclei which are bound nuclear systems with hyperon(s) since a direct reaction experiment with either/both hyperon targets or/and beams is impractical because of short lifetimes of hyperons, an order of 100 ps. Structures of hypernuclei and their decay have been studied for more than four decades, however, the information on hypernuclei is yet limited, and the total number of hypernuclei investigated so far is not large. Furthermore, the investigation on hypernuclei has mainly been performed on or in adjacent to the β -stability line because hypernuclei were produced with a stable target material using meson beams. There are only very scarce data on Λ -hypernuclei with nucleonic cores far from the β -stability line (we call them **exotic hypernuclei**). The region of the nuclear chart far from the β -stability line in the strangeness $S = -1$ sector is still *terra incognita*. Information on very neutron rich hypernuclei is essential to understand the nature of neutron stars, however, such neutron rich hypernuclei have never been produced yet. Another important piece of information are hypernuclear magnetic moments, which will contribute to the understanding of hyperon-nucleon interactions on the quark level. They are very difficult to be measured by meson and electron beam induced spectroscopy. In the coming decade the field of hypernuclear physics is entering a new era with a number of international experiments such as FINUDA at the DAΦNE accelerator facility at Frascati [1], HKS in CEBAF [2], KaoS at MAMI C [3], J-PARC [4, 5] and PANDA at FAIR [6]. These experiments can reach variety of physics, however, exotic hypernuclei and hypernuclear magnetic moments can not be reached by these experiments. Therefore, the international HypHI collaboration has submitted a Letter-Of-Intent of “Hypernuclei with Stable Heavy Ion Beam and RI-beam Induced Reactions at GSI (HypHI)” [7] to the GSI spring PAC EA 30 in 2005 in order to study exotic hypernuclei and hypernuclear magnetic moments with heavy ion induced reactions at GSI and FAIR, and it has been already discussed by the GSI PAC as LOI40. As described in LOI40 [7], the physics subjects of the HypHI project are

- Hypernuclei toward the proton and neutron drip-lines,
- Magnetic moments of hypernuclei,
- $\Lambda - \Sigma$ coupling in the nuclear matter,
- Decay of exotic hypernuclei,
- Charge symmetry breaking in ΛN interaction,
- Coulomb dissociation of loosely-bound hypernuclei,
- Measurements of the binding energy of exotic hypernuclei. It was not mentioned in LOI, however, it is realized to be possible to measure because of reasonable invariant mass resolution expected in according to Monte Carlo simulations.

Hypernuclear production via a heavy ion collision was first theoretically studied by Kerman and Weiss [8]. They pointed out that it is only the way to produce hypernuclei with several hyperons and other exotic strange nuclei. In high energy heavy ion collisions, it is well known that the participant-spectator model explains the general feature of the reaction. The overlapped region between the two nuclei (participants) participates in the collision, while the nucleons in the off-overlapping region (spectators) pass by each other without experiencing a large disturbance. Hyperons such as Λ are produced in the participants region at

around the mid-rapidity. Because of their wide rapidity distribution, one may produce a hypernucleus with a coalescence of hyperon(s) in the projectile fragments, thus the velocity of hypernuclei is close to the one of projectile. Because of the energy threshold of ~ 1.6 GeV for Λ production of an elementary process of $NN \rightarrow \Lambda KN$, the produced hypernuclei have a large velocity with $\beta > 0.9$ and their effective lifetime is longer than at rest because of a large Lorentz factor. Decays of hypernuclei can be studied in-flight, and most of their decay vertices are a few tens of centimeters behind the target at which hypernuclei are produced. In the late 80s, hypernuclear production with heavy ion beams was performed in Dubna [9, 10] with beams of 3.7 A GeV ${}^4\text{He}$ and 3.0 A GeV ${}^7\text{Li}$ impinging on a polyethylene target. They deduced a production cross section for ${}^4_{\Lambda}\text{H}$ as $\sim 0.3 \mu\text{b}$, which was reproduced by the theoretical calculation based on a model of a Λ coalescence in projectiles [11, 12]. Recently, ${}^3_{\Lambda}\text{H}$ has also been produced and identified with central 11.5 A GeV/c Au+Pt collisions by the BNL AGS E864 collaborations [13]. Even though the two experiments at JINR and BNL have shown the production of hypernuclei with heavy ion beams, the feasibility of the reliable hypernuclear spectroscopy with heavy ion beams has not been yet proven, and the answer to questions on the feasibility has to be given experimentally.

Therefore, the HypHI collaboration proposed to G-PAC 33 a pilot experiment of the HypHI project [14], which we define as Phase 0, in order to investigate the feasibility of hypernuclear spectroscopy with heavy ion beams. The main aim of the proposed experiment is to confirm the experimental evidence at JINR in the late 80's of the production of ${}^3_{\Lambda}\text{H}$, ${}^4_{\Lambda}\text{H}$ and ${}^5_{\Lambda}\text{He}$ with ${}^6\text{Li}$ beams impinging on a ${}^{12}\text{C}$ target at 2 A GeV. In the Phase 0 experiment, the following experimental information could be obtained;

- Cross section for production of the ${}^3_{\Lambda}\text{H}$, ${}^4_{\Lambda}\text{H}$ and ${}^5_{\Lambda}\text{He}$ hypernuclei,
- Lifetimes of ${}^3_{\Lambda}\text{H}$, ${}^4_{\Lambda}\text{H}$ and ${}^5_{\Lambda}\text{He}$,
- Polarization of hypernuclei produced in heavy ion collisions,
- Coalescence mechanism in fragmentation reactions,
- Other information, like the forward correlation among hyperons and nucleons.

G-PAC 33 discussed on the HypHI Phase 0 proposal, and it has granted seven night shifts for the test of the trigger system and detectors. However, the requested 45 shifts for the Phase 0 experiment have not been approved. In the letter from G-PAC 33, the event generator for the HypHI Monte Carlo simulations with the UrQMD calculations [15] was discussed, and further experimental investigations on the first level trigger, the tracking trigger, were suggested. The HypHI collaboration took recommendations from G-PAC 33 seriously, and we performed further investigations. Since the tracking trigger is made from scintillating fiber detectors together with newly developed VME logic modules, prototypes of scintillating fiber detectors and logic modules have been tested in the laboratories by using cosmic-rays, β -radiation sources, laser pulses and test signals. A part of results of the laboratory test will be shown in the next section. The HypHI collaboration has also spent three shifts of beam times in March 2007 in order to test prototypes of fiber detectors, VME logic modules and a diamond detector with ${}^{12}\text{C}$ beams at 2 A GeV and π^+ cocktail beams at 3.3 Tm. In addition to the detector tests, the most important algorithm for the tracking trigger, the on-line clustering by logic modules, has been tested. We have also investigated further on possible event generators for the Monte Carlo simulation. With this progress report, the HypHI collaboration would like to answer to all the suggestions and criticisms in the letter from G-PAC 33 in order to let the HypHI Phase 0 experiment fully be approved by G-PAC 34.

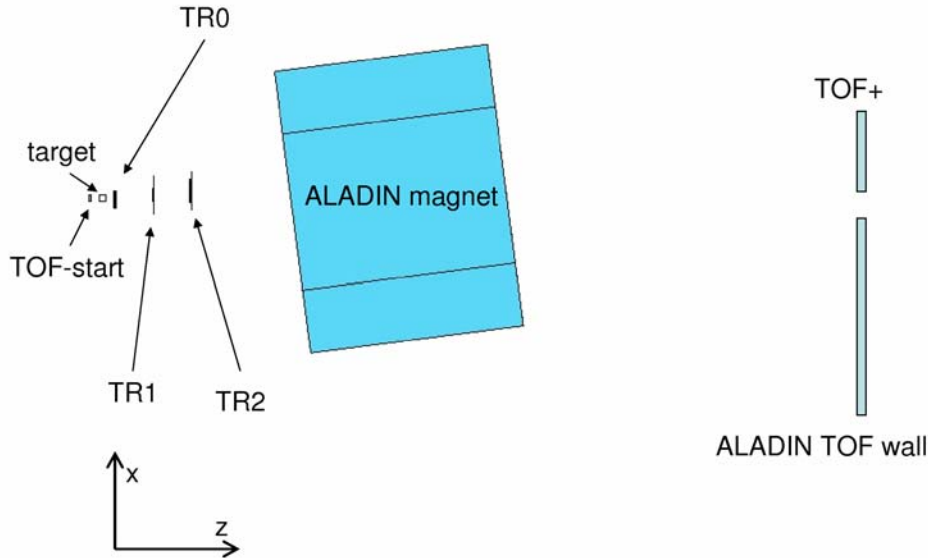


Figure 1: A schematic drawing of the proposed experimental setup for the Phase 0 experiment in cave C. The same setup was discussed in the HypHI Phase 0 proposal [14].

The HypHI project has been already approved by the Helmholtz Association as the Helmholtz-University Young Investigators Group (YIG) VH-NG-239 with Mainz University, and the supported new group at GSI is led by the HypHI spokesperson, T.R. Saito. The funding from the Helmholtz Association and GSI for five years has been already started since April 2006. The GSI YIG group recently got an approved DFG research grant for the development of a TOF wall for positively charged particles, TOF+, with 180 k Euro investment budget and one postdoc positions for two years.

2 Progress of developments for detectors and trigger systems

Figure 1 shows a proposed setup of the HypHI Phase 0 experiment, which has already discussed in the proposal [14]. The proposed setup consists of a ^{12}C target with a thickness of 8 g/cm^2 , the ALADiN dipole magnet, a diamond detector, three scintillating fiber detectors, TR0, TR1 and TR2, two Time-Of-Flight (TOF) walls, the ALADiN TOF wall for negatively charged particles and TOF+ for positively charged particles. There will be additional detectors, a K^+ detector on the side wall in the cavity of the ALADiN magnet to confirm strangeness productions by measuring K^+ and two sets of drift chambers from KEK. The trigger system to the data acquisition consists of three levels, the tracking trigger, the π^- trigger and the $Z = 2$ trigger as discussed in the HypHI Phase 0 proposal [14].

After G-PAC 33 in 2006, there have been several progress on the developments of detectors and trigger systems. In the following sub-sections, the progress on the scintillating fiber detectors, the tracking trigger, TOF+ and drift chambers will be presented.

2.1 Scintillating fiber detectors and tracking trigger

For the scintillating fiber detectors, TR0, TR1 and TR2, Kuraray SCSF-78 scintillating fibers with an outer diameter of 0.83 mm and an active core of 0.73 mm will be used. This

type of fiber has a short decay constant of 2.8 ns and a long attenuation length of more than 4 m. Prototypes which were tested in the laboratory and with beams consists of 2- and 4- layers of fibers at a pitch of 0.59 mm. For simplicity the fibers have been oriented perpendicular to the beam axis. A prototype from the Osaka Electro-Communication University (OECU) consists of two-layers with 64 channels, while a prototype from the Mainz University consists of 4-layers with 32 channels. The read-out of scintillating photons is performed with the Hamamatsu Photonics H7260 multi-anode photomultiplier tubes. There are two types of H7260, a commercial H7260K and an improved version, H7260KS, with less cross-talks achieved by placing grids in the front-glass window between each photo-cathode channel. Both of the types of photomultipliers were tested in the laboratory and with beams, and the results will be discussed in the next subsections.

In the final design of TR0, TR1 and TR2, analog signals from the photomultipliers are processed by a discriminator card developed by the MAMI C KaoS collaboration with a chip of 4 integrated low walk double-threshold discriminators (DTDs), the GSI-chip3. Approximately 1200 channels of the discriminators will be prepared by the Mainz University by the end of 2007, and several prototypes will be available soon. LVDS logic signals from the discriminator board will be guided to a FPGA based logic module (VUPROM) which is developed for the HypHI project at GSI. The time measurement for the scintillating fiber arrays will be performed in the logic module, based on the FPGA logic calculation with 400 M Hz clocks, providing a granularity of the time measurement of 2.5 ns. The basic design of VUPROM has been already done by Jan Hoffmann of the GSI Experiment Electronics department. Each VUPROM module has 256 channels I/O with an LVDS standard and is equipped with an FPGA with 400 M Hz and a DSP with 1 G Hz. Twenty five modules will be produced in 2007. A prototype of VUPROM, which is referred to as VULOM, is already available to the HypHI project, and it has been tested in the laboratory with test signals and at cave A with beams for the TDC and scaler functions as well as for the tracking trigger. The results of the tests will be also presented in the next subsections.

For TR0, an additional analog readout will be performed by CAEN VME QDCs in order to distinguish ${}^3_{\Lambda}\text{H}$ and ${}^4_{\Lambda}\text{H}$ from background containing α -particles produced at the target. As discussed in the proposal [14], it will play an essential role for the selection of hydrogen hypernuclei. The energy resolution of the prototypes of scintillating fiber detectors with the QDC has been already investigated with cosmic-rays, β -radiation sources and beams, the detail of which will also be presented in the next sub-sections.

2.1.1 Tests with cosmic-rays, radiation sources and lasers

A prototype of fiber detectors from Osaka Electro-Communication University (OECU prototype) has been tested with cosmic rays and β -rays from the ${}^{90}\text{Sr}$ radiation source in order to investigate the response and energy resolution of the detector for minimum ionizing particles. The OECU prototype consists of two-layers of fibers with a total of 64 channels. The half of the fiber detector was connected to a photomultiplier H7260KS with a suppression of cross-talk. Analog signals were directly processed by VME charge sensitive ADCs (QDCs). Measurement with both cosmic-rays and β -rays were performed with a coincidence measurement by additional plastic scintillator placed just below the fiber detector. Figure 2 shows a typical raw spectrum of one of the fiber channels with cosmic-rays. A high narrow peak at lower channels corresponds to pedestal currents in the electronics, and a wider peak at larger channels around at 150 is due to the energy deposit of cosmic rays in the detector. The peak of cosmic-rays is well separated from the pedestal peak, which shows a capability of the OECU prototype to measure minimum ionizing particles. However, since the amplitude of the cosmic-ray signals is rather small, the result of these measurements have suggested to

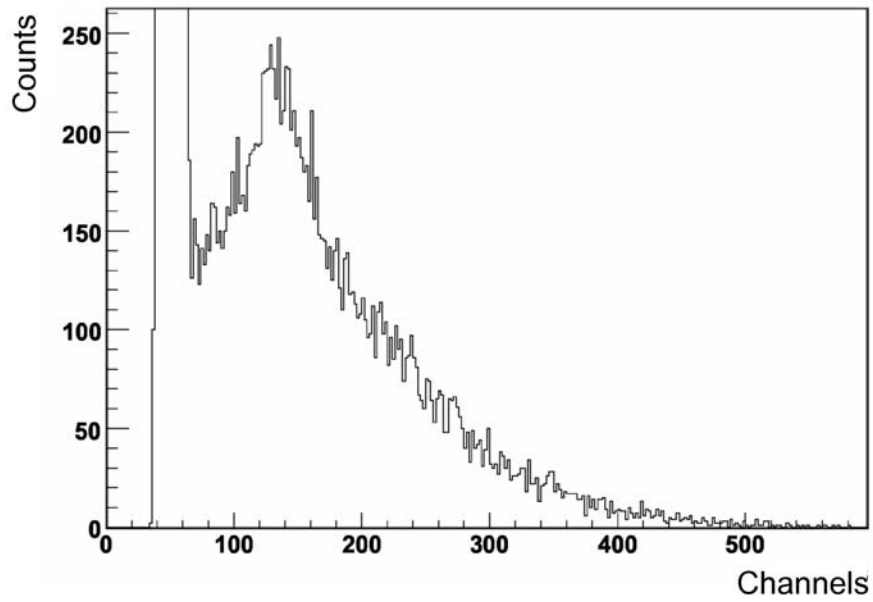


Figure 2: A typical raw QDC spectrum of one of the channel of the OECU prototype of fiber detectors with cosmic-rays.

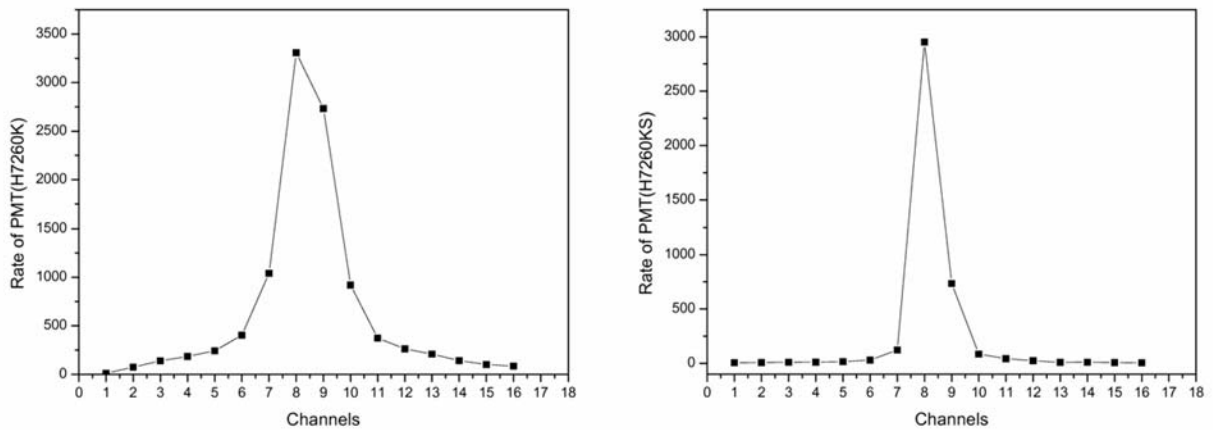


Figure 3: Distribution of observed rates of a half of H7260K (left) and H7260KS (right). A fiber is connected to the channel 8, and an intense laser illuminate only the fiber. The level of cross-talk is drastically reduced for H7260KS.

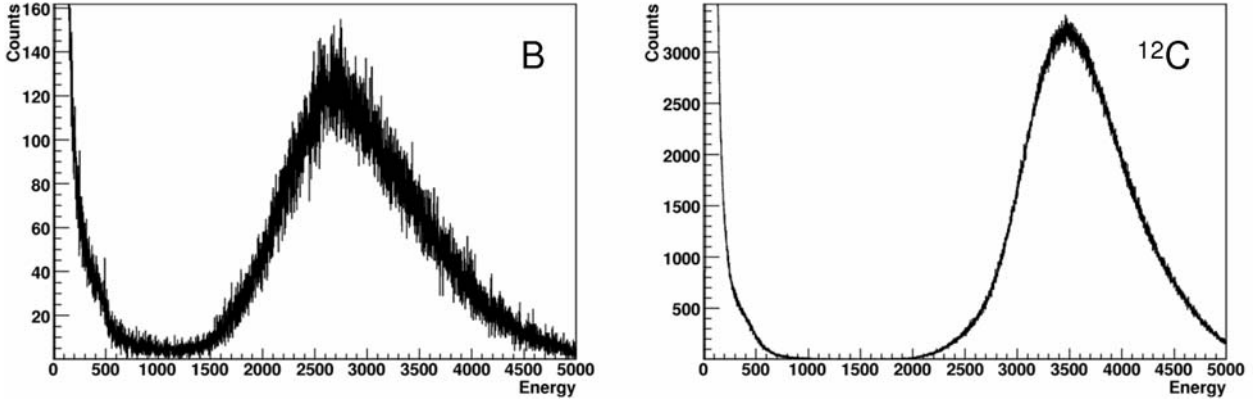


Figure 4: Energy deposit distribution for the Mainz fiber prototype with H7260K by using ^{12}C beams on a ^{12}C target with selections of outgoing B isotopes (left) and ^{12}C (right).

have 4 fiber-layers for all the TR0, TR1 and TR2.

For reasonably good tracking triggers made from scintillating fiber detectors, the suppression of a cross-talk in the neighboring channels is very crucial. Since the cross talk is mainly induced inside multi-anode photomultipliers, the cross-talk response of the photomultipliers were tested. Two different types of multi-anode photomultipliers were tested, a commercial 32-anode photomultiplier H7260K and an improved version H7260KS for lower cross-talks. H7260KS has grids in the grass window in front of the photo-cathodes to separate pixels. A single fiber is attached to the channel 8 of the both photomultipliers, and the fiber is illuminated by laser photons. The other channels were shielded well from the laser illuminations. In the measurement, the threshold level of a discriminator module was below the single photoelectron amplitude. Figure 3 shows an observed rate from channels 1 through 16 for H7260K (left) and H7260KS (right). In the both distribution, the channel 8 which is connected to the single fiber has the highest amplitude, however, a significant difference on the width of the distribution is observed. It shows that the probability of cross-talk with H7260KS is significantly lower, and it meets the requirement from the tracking trigger. Therefore, H7260KS will be used for all the scintillating fiber detector TR0, TR1 and TR2.

2.1.2 Test with ^{12}C beams at 2 A GeV and cocktail beams at 3.3 Tm

In March 2007, a test experiment was performed at cave A by spending three of seven night shifts which were granted by G-PAC 33. The goal of the test experiment was to test the OECU fiber prototype detector and another prototype from Mainz University with 4 fiber layers as well as the prototype of VUPROM logic modules, VULOM, for the tracking trigger. A carbon target with a thickness of 4 cm can be also mounted. The distances from the target to the OECU and Mainz prototypes are respectively 40 and 70 cm. Readout of scintillating photons from fibers were performed by H7260KS for the OECU prototype and H7260K for the Mainz prototype. For the OECU prototype, both the analog and logic signals were processed by a CAEN VME QDC and VULOM, respectively, while for the Mainz prototype, only analog signals were processed by a CAEN VME QDC. For the OECU prototype, logic signals of a few channels were also readout by a CAEN VME TDC in order to check the TDC function implemented in VULOM. In addition to the fiber detectors, one detector with a single fiber with a two-inch PMT and a diamond detector with an area of 1 cm^2 was mounted behind the Mainz prototype. Additional two plastic scintillators were mounted each in front of the target and behind the diamond detector for TOF measurements

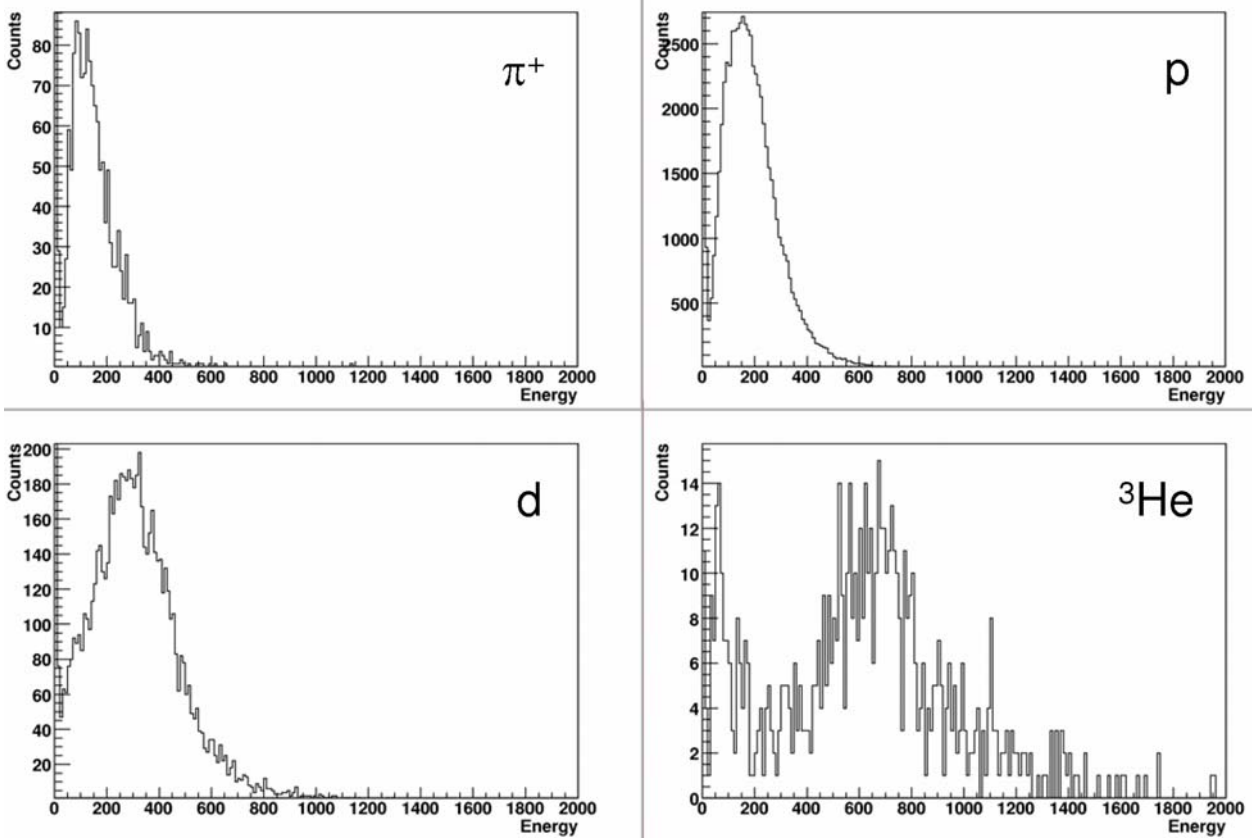


Figure 5: Energy deposit distribution for the OECU fiber prototype with H7260KS by using cocktail beam at 3,3 Tm with selections of π^+ (top left), proton (top right), deuteron (bottom left) and ^3He (bottom right) beams.

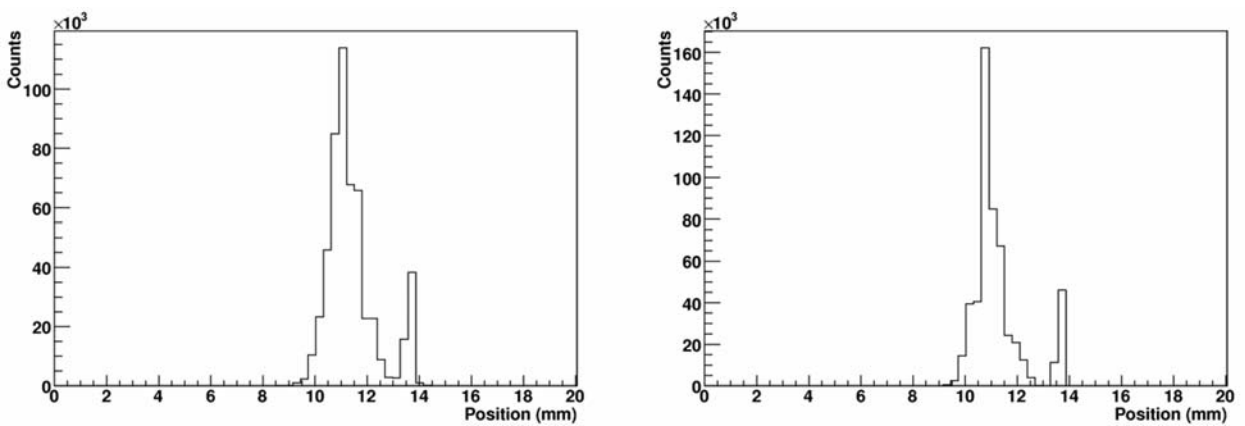


Figure 6: Distribution of rates in the OECU fiber prototype by requiring a coincidence with a hit in a single fiber detector 40 cm behind the prototype and a small diamond detector 1 m behind the prototype. The left panel corresponds a distribution of rates by the TDC data, and the right one is with a weighted average of the QDC data.

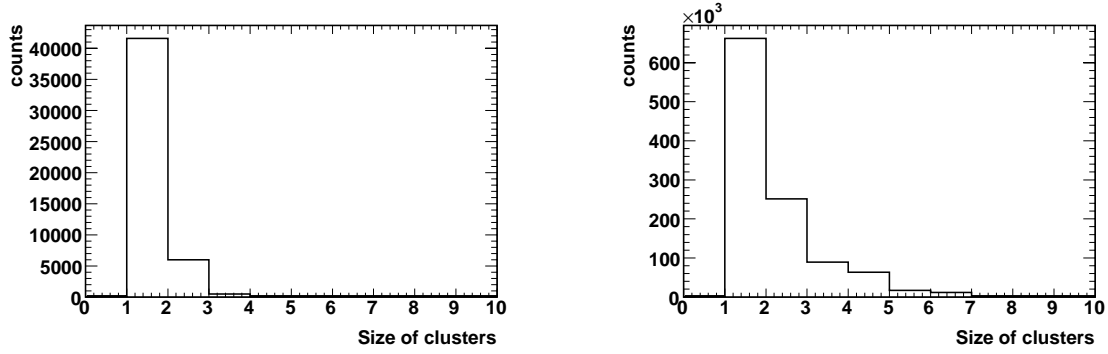


Figure 7: Size of clusters measured with ^{12}C beam (right) and the π^+ beams in cocktail beams (left)

with a distance of 2.4 m between them. Signals from the plastic scintillator in front of the target were used as trigger to the data acquisition system. For the study of energy resolution of the fiber detectors, since the OECU prototype is equipped with charge sensitive amplifiers of a gain of 10, the OECU prototype is used to investigate the energy resolution of light charged particles up to $Z = 2$ and the Mainz one for heavier charged particles such as B and ^{12}C . It should be noted that all the detectors were mounted in the air.

The SIS accelerator delivered ^{12}C beams at 2 A GeV to cave A. The carbon beams were impinged on the carbon target in cave A to produce secondary particles. The charge of the secondary particles was selected in the analysis for ΔE (stop-counter) event by event. Defocused beams without target also illuminate the whole fiber detectors in order to perform the gain matching of each fiber channels. For the data analyses, fired neighboring channels were clustered, and the energy deposit was properly summed in the cluster with the gain matching. The right panel of Figure 4 shows the energy deposit spectrum of the Mainz prototype for the primary ^{12}C beam. The width of the distribution in RMS is approximately 15 % which fulfill the requirement of the energy resolution for TR0. With the ^{12}C beam, secondary B beams from the carbon target were selected by the ΔE analysis, and the energy deposit distribution of the Mainz prototype for the B beams is shown in the left panel of the figure. It is observed that these two distributions are well distinguished. The observed energy deposit distribution for B is wider than that of ^{12}C because the B beams are secondary produced at the carbon target with a wider momentum distribution.

The primary ^{12}C beam was also impinged on a pion production target made of Be in the pion beam line, and a secondary cocktail beam with π^+ , proton, deuteron, triton and ^3He at 3.3 Tm was delivered to cave A. Each beam particle was analyzed event by event by TOF- ΔE . With the cocktail beam, the response of the OECU prototype was studied for π^+ , proton, deuteron and ^3He secondary beams. Figure 5 shows the energy deposit distribution of the OECU prototype for π^+ (top-left), proton (top-right), deuteron (bottom-left) and ^3He (bottom-right). It shows an excellent sensitivity of the fiber detectors for light charged particles even for π^+ . A separation of ^3He from protons at 3.3 Tm is also shown in the figure. It shows that the proposed fiber detectors have already fulfilled the requirements for the Phase 0 experiment for the energy response.

The position resolution of the OECU prototype was also investigated by requiring a coincidence measurement of the primary ^{12}C beam by the single-fiber detector and the diamond detector placed behind the Mainz prototype. Figure 6 shows the distribution of the central position of the cluster for the OECU prototype only with the TDC data from VULOM (left

panel) and with a weighted average by additional QDC data (right panel). A spike around at 13.5 in the both panel corresponds to one noisy channel. The highest peaks are showing the position resolution in this method, and a RMS width for the peaks in the left and right panels is respectively 0.62 and 0.54 mm, which also fulfills the requirements for the tracking accuracy. In the measurements, there is also an ambiguity for the thickness and alignment of the single-fiber detector, therefore, the real position resolution is expected to be slightly better.

The tracking trigger, which is made with the scintillating fiber detectors and newly developed VME universal processing modules (VUPROM) by requesting the existence of a secondary decay vertex behind the target is the most essential part for the Phase 0 experiment. A part of functions of the tracking trigger has been implemented on-board with a prototype of VUPROM, VULOM, and it has been tested in the experiment at cave A in March 2007. The analog signals from the OECU prototype are fed to VME leading edge discriminator modules (update type for the output signals), and the logic signals from the discriminator modules are processed by VULOM. The algorithm to create the tracking trigger by FPGA in the final stage could be as follows;

- (1) Define the hit position of each particle in TR0, TR1 and TR2,
- (2) Find tracks from the primary vertex at the target by matrix coincidences,
- (3) Veto the tracks from the primary vertex,
- (4) Find tracks from the secondary decay vertex by matrix coincidences.

The most crucial part in the tracking trigger algorithm is the procedure (1) since each charged particle penetrates in the fiber planes fire not only one channel of the fiber detector but several neighboring channels. Therefore, the neighboring hit has to be treated as one single hit, which is so called “clustering”. This is one of the challenges in the tracking trigger, and the clustering function was tested in the beam time.

The clustering function implemented in VULOM packs up to six neighboring fired channels into one cluster and gives the center of the cluster as a hit position. A cluster with a size larger than six was ignored, which was optimized by the Monte Carlo simulations. It is important to observe experimentally a typical cluster size because there may be some effects which are not taken into account for in the simulations. Figure 7 shows measured cluster size with VULOM with the ^{12}C and the π^+ beam in the cocktail beam. It shows that accepting clusters with the size of up to 5 seems sufficient.

Table 1 shows a typical event processed by VULOM. The first and second columns are respectively the channel ID and the TDC value measured by VULOM. The third column shows the pulse amplitude measured by a CAEN VME QDC after the pedestal subtraction. In the fourth column a waveform of the raw signals by binary for 240 ns is shown. Each bit corresponds to a duration of 10 ns. Time is processed from left to right. The fifth and sixth columns show respectively the cluster center and the waveform of the cluster. In the event shown in Table 1, channels 16, 17, 18, 20 and 21 are fired by the TDC data. It is also consistent to the QDC data except for the channel 21. After the clustering by coincidences for the waveform, there are two cluster observed at the position at 17 and 20.5. For the both cases, it is demonstrated that the on-line clustering is working correctly.

For the TDC function implemented in VULOM, a time distance of signals into each input channel to the trigger signal as a common-stop made from the signal from the start counter for TOF is measured with a time granularity of 2.5 ns. A TDC distribution taken by the logic module is shown in the bottom panel in Figure 8. The TDC data taken by VULOM are compared by the data taken by a CAEN VME TDC, as shown in the top-left panel in

Table 1: A typical event processed by VULOM. The first and second columns are respectively the channel ID and the TDC value measured by the logic module. The third column shows the pulse amplitude measured by a CAEN VME QDC after the pedestal subtraction. In the fourth column a waveform of the raw signals by binary for 240 ns is shown. Each bit corresponds to a duration of 10 ns. Time is processed from left to right. The fifth and sixth columns show respectively the cluster center and the waveform of the cluster. Channels 16, 17, 18, 20 and 21 are fired by the TDC data. It is also consistent to the QDC data except for the channel 21. After the clustering by coincidences for the waveform, there are two cluster observed at the position at 17 and 20.5.

Fiber ID	TDC	Amplitude	Raw waveform	Position	Clustered waveform
0	0	-20.3	00000000000000000000000000000000	0.0	00000000000000000000000000000000
1	0	-9.5	00000000000000000000000000000000	0.5	00000000000000000000000000000000
2	0	-24.1	00000000000000000000000000000000	1.0	00000000000000000000000000000000
3	0	-15.6	00000000000000000000000000000000	1.5	00000000000000000000000000000000
4	0	-19.2	00000000000000000000000000000000	2.0	00000000000000000000000000000000
5	0	0.0	00000000000000000000000000000000	2.5	00000000000000000000000000000000
6	0	-8.7	00000000000000000000000000000000	3.0	00000000000000000000000000000000
7	0	-1.6	00000000000000000000000000000000	3.5	00000000000000000000000000000000
8	0	0.0	00000000000000000000000000000000	4.0	00000000000000000000000000000000
9	0	-9.0	00000000000000000000000000000000	4.5	00000000000000000000000000000000
10	0	-0.3	00000000000000000000000000000000	5.0	00000000000000000000000000000000
11	0	0.3	00000000000000000000000000000000	5.5	00000000000000000000000000000000
12	0	-14.7	00000000000000000000000000000000	6.0	00000000000000000000000000000000
13	0	-6.6	00000000000000000000000000000000	6.5	00000000000000000000000000000000
14	0	-1.8	00000000000000000000000000000000	7.0	00000000000000000000000000000000
15	0	-8.2	00000000000000000000000000000000	7.5	00000000000000000000000000000000
16	59	84.5	00000001111100000000000000000000	8.0	00000000000000000000000000000000
17	60	487.3	00000001111111110000000000000000	8.5	00000000000000000000000000000000
18	60	456.4	00000001111100000000000000000000	9.0	00000000000000000000000000000000
19	0	-2.7	00000000000000000000000000000000	9.5	00000000000000000000000000000000
20	59	141.4	00000001111100000000000000000000	10.0	00000000000000000000000000000000
21	59	0.4	00000001111100000000000000000000	10.5	00000000000000000000000000000000
22	0	0.1	00000000000000000000000000000000	11.0	00000000000000000000000000000000
23	0	18.3	00000000000000000000000000000000	11.5	00000000000000000000000000000000
24	0	-7.4	00000000000000000000000000000000	12.0	00000000000000000000000000000000
25	0	0.0	00000000000000000000000000000000	12.5	00000000000000000000000000000000
26	0	23.0	00000000000000000000000000000000	13.0	00000000000000000000000000000000
27	0	0.3	00000000000000000000000000000000	13.5	00000000000000000000000000000000
28	0	-0.1	00000000000000000000000000000000	14.0	00000000000000000000000000000000
29	0	-0.8	00000000000000000000000000000000	14.5	00000000000000000000000000000000
30	0	5.3	00000000000000000000000000000000	15.0	00000000000000000000000000000000
31	0	4.5	00000000000000000000000000000000	15.5	00000000000000000000000000000000
				16.0	00000000000000000000000000000000
				16.5	00000000000000000000000000000000
				17.0	00000001111111110000000000000000
				17.5	00000000000000000000000000000000
				18.0	00000000000000000000000000000000
				18.5	00000000000000000000000000000000
				19.0	00000000000000000000000000000000
				19.5	00000000000000000000000000000000
				20.0	00000000000000000000000000000000
				20.5	00000001111100000000000000000000
				21.0	00000000000000000000000000000000
				21.5	00000000000000000000000000000000
				22.0	00000000000000000000000000000000
				22.5	00000000000000000000000000000000
				23.0	00000000000000000000000000000000
				23.5	00000000000000000000000000000000
				24.0	00000000000000000000000000000000
				24.5	00000000000000000000000000000000
				25.0	00000000000000000000000000000000
				25.5	00000000000000000000000000000000
				26.0	00000000000000000000000000000000
				26.5	00000000000000000000000000000000
				27.0	00000000000000000000000000000000
				27.5	00000000000000000000000000000000
				28.0	00000000000000000000000000000000
				28.5	00000000000000000000000000000000
				29.0	00000000000000000000000000000000
				29.5	00000000000000000000000000000000
				30.0	00000000000000000000000000000000
				30.5	00000000000000000000000000000000
				31.0	00000000000000000000000000000000
				31.5	00000000000000000000000000000000

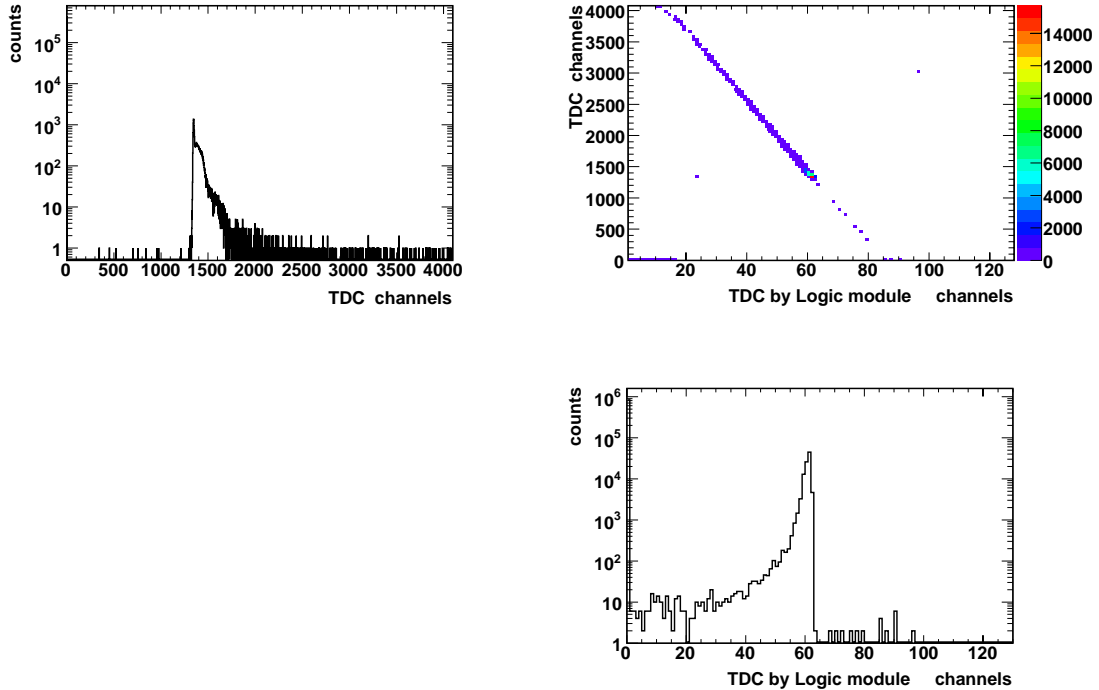


Figure 8: A TDC histogram obtained by the TDC function of the logic module (bottom). A TDC histogram taken by a CAEN VME TDC for the same channel is also shown in the top-left panel. In the top-right panel, a correlation between the TDC data taken by the logic module and CAEN TDC is shown.

the figure. In the top-right panel, a correlation between the TDC data taken by VULOM and CAEN TDC is shown. It shows an excellent linear correlation demonstrating that the TDC function is working properly. Tails shown in the both TDC distributions correspond to the walk effect in leading edge discriminator modules.

As a summary of this subsection, it is observed that the prototypes of fiber detectors have shown their capability to measure positions and energy deposits of charged particles from π^+ to ^{12}C by fulfilling the requirements for the Phase 0 experiment. The prototype of the logic modules, VULOM, and the algorithms have also demonstrated the feasibility of the tracking trigger by performing proper on-line clustering and TDC functions.

2.1.3 Final design of scintillating fiber detectors

By the investigations on the prototypes of scintillating fiber detectors together with Monte Carlo simulations, the final design of the arrays of scintillating fiber detectors, TR0, TR1 and TR2 was finally fixed. All of the fiber layers consist of 4-layers of scintillating fibers which are connected to HAMAMATSU photomultipliers H7260KS. The HypHI collaboration together with HAMAMATSU designed a new high-voltage base with three booster cables to stabilize the voltage in the last three dinode sections, and it will be used for all the photomultipliers. Ten photomultipliers have been already purchased by Osaka University and Osaka Electro Communication University. Table 2 summarizes the specification of TR0, TR1 and TR2. The y -layers of TR1 and TR2 are purchased by Osaka Electro-Communication University, and they will be delivered soon to GSI for further tests. Electronics modules and photomultipliers associated to TR0 will be purchased by the DFG research grant to TOF+, which also granted the budget for TR0.

Table 2: Specification of scintillating fiber detectors, TR0, TR1 and TR2.

		Layers	Size [cm]	Channels	Number of H7260KS
TR0	x	4	3.8	64	2
	y	4	3.8	64	2
TR1	x	4	13.2	224	7
	y	4	7.6	128	4
TR2	x	4	24.5	416	13
	y	4	11.3	192	6

2.1.4 Development and production of new VME logic modules for the tracking trigger

With tests of prototypes, VULOM, for the tracking trigger, the final design of the new module, VUPROM, has been made. Each module is equipped with a 400 MHz FPGA and a 1 GHz DSP. Each VUPROM module has 256 channels I/O. Input signals can be either ECL or LVDS and the output signals are LVDS. The first five modules will be delivered by May and additional 25 modules will be produced by summer 2007.

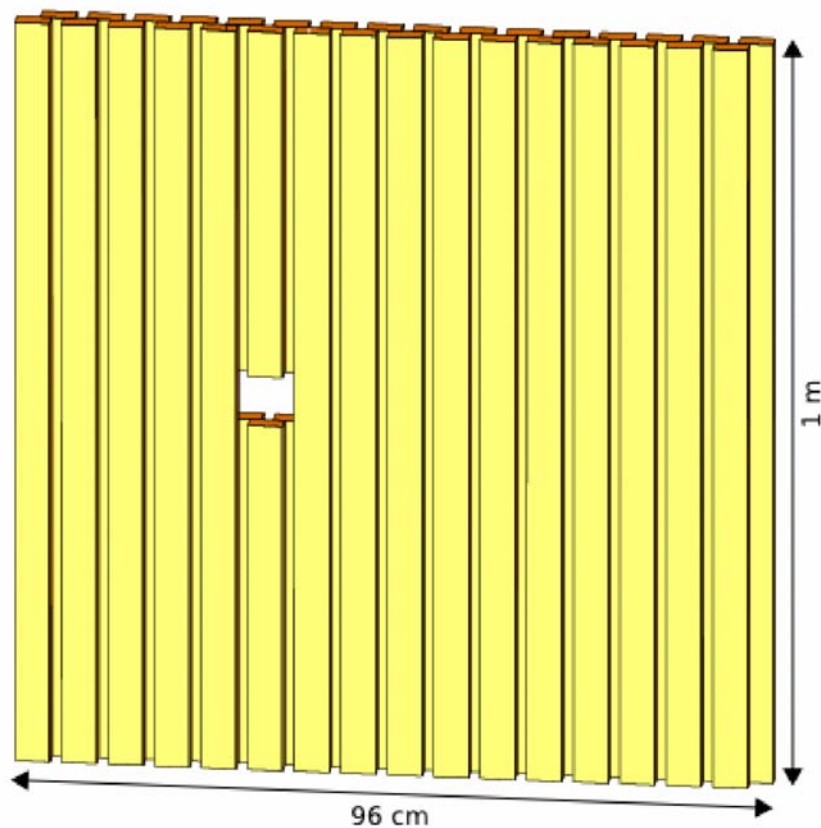


Figure 9: Plastic scintillator bars of TOF+.

2.2 TOF+: a TOF wall for positively charged particles

Positively charged particles are bent upwards in Figure 1, and they are measured by a detector, indicated as TOF+ in the figure. TOF+ consists of plastic scintillator bars mounted along the y axis in the xy -plane, which is similar to the ALADiN TOF wall. The requirements for TOF+ are;

- Time and energy resolution good enough to identify particles with $Z=1, 2$ and 3 ,
- Counting rate per bar should be less than 1 MHz with a primary beam of ${}^6\text{Li}$ at 10 MHz on a carbon target with a thickness of 8 g/cm^2 ,
- Reasonable position resolution for an order of centimeters for tracking charged particles,
- Large acceptance to detect protons and α -particles from ${}^3_\Lambda\text{H}$, ${}^4_\Lambda\text{H}$ and ${}^5_\Lambda\text{He}$ hypernuclei.

Figure 9 shows the layout of plastic scintillator bars in TOF+. By the requirement for the counting rate, a width of plastic scintillators as 4.5 cm is chosen with a thickness of 2.5 cm in order to achieve a reasonable good energy resolution. Neighboring bars are overlapped by 1.5 cm, thus a position granularity is 1.5 cm. The length of the bar is 1 m, and the horizontal size of the whole TOF+ array is 0.96 m. Three bars around at the beam trajectory are divided into two pieces in order to form a hole with a size of $7.5 \times 6.5 \text{ cm}^2$ for the beams. With this geometry, an acceptance for protons and α -particles from the decay of ${}^5_\Lambda\text{He}$ is 97.2 % and 93.1 %, respectively. Readout of scintillating light is performed at both ends with the photomultipliers HAMAMATSU R3478, the same type as used in the ALADiN TOF wall. Both energy and time information is measured with CAEN VME QDC and TDC (time to digital converter), respectively.

Monte Carlo simulations for ${}^4_\Lambda\text{H}$ hypernuclei has been re-performed by using the current geometry of TOF+. Events including ${}^4_\Lambda\text{H}$ hypernuclei with the UrQMD calculations were used for the simulations with all the associated particles. In the current Monte Carlo simulations, a calculated field map for the ALADiN magnet without field clamps is used for simulating events, and the analysis of the simulated events were performed with a well-like field distribution with a sharp boundary. In the Monte Carlo simulations presented in the proposal [14], a well-like magnetic field distribution was used also to simulate events. Figure 10 shows correlations between simulated momenta and reconstructed momenta with the current setup for α -particles (top left) and π^- (bottom left) from the decay of ${}^4_\Lambda\text{H}$. In the right panels, distributions of difference between reconstructed and simulated momentum are shown for α -particles (top right) and π^- (bottom right) from the decay of ${}^4_\Lambda\text{H}$. Momentum resolution of α -particles and π^- from the decay of ${}^4_\Lambda\text{H}$ are $0.33 \text{ GeV}/c$ and $0.01 \text{ GeV}/c$, respectively. The acceptance for the coincident measurement of π^- and for α -particles from the decay of ${}^4_\Lambda\text{H}$ is as large as the value presented in the proposal [14], approximately 20 %, which is mainly dominated by the acceptance for π^- because of small momenta of π^- . Invariant mass of ${}^4_\Lambda\text{H}$ has been also reconstructed in the similar manner presented in the proposal [14]. Figure 11 shows a distribution of the reconstructed invariant mass for ${}^4_\Lambda\text{H}$ with the current setup. A mass resolution of $3.15 \text{ MeV}/c^2$ has been deduced by Gaussian fitting for ${}^4_\Lambda\text{H}$. The efficiency to reconstruct ${}^4_\Lambda\text{H}$ is approximately 2.4 % with associated particles even though the acceptance for ${}^4_\Lambda\text{H}$ events is about 20 %. This loss is due to tight cut conditions in the analysis and due to mistracking in the current setup. The efficiency will be increased by having more redundancy of the tracking system by mounting drift chambers between TR1 and TR2 and at the exit of the ALADiN magnet, which will be discussed in the next sub-section. It should be noted that the number of reconstructed events has remained

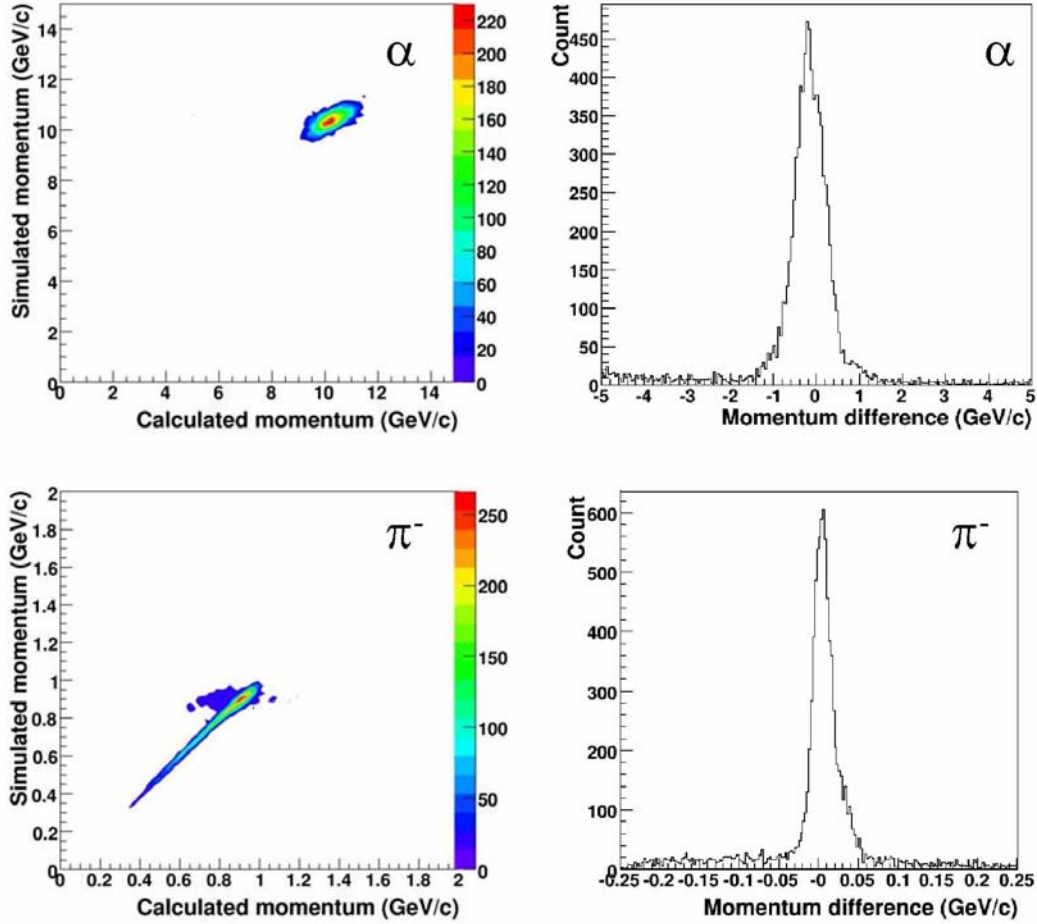


Figure 10: Correlations between simulated momenta and reconstructed momenta with the current setup for α -particles (top left) and π^- (bottom left) from the decay of ${}^4_{\Lambda}\text{H}$. In the right panels, distributions of difference between reconstructed and simulated momenta are shown for α -particles (top right) and π^- (bottom right) from the decay of ${}^4_{\Lambda}\text{H}$. Momentum resolution of α -particles and π^- from the decay of ${}^4_{\Lambda}\text{H}$ are 0.329 GeV/c and 0.010 GeV/c, respectively.

very similar to the one presented in the proposal [14].

The GSI YIG group is granted by DFG for the development and construction of TOF+ with an investment budget of 180 k Euro and one postdoc position for two years, and the grant will be available as soon as the proposal of the Phase 0 experiment is approved.

2.3 Drift chambers

In the current consideration of the experimental setup for the Phase 0 experiment, two sets of drift chambers from KEK in Japan are considered in order to increase the redundancy of the tracking. The specification of the drift chambers is summarized in Table 3. In the table, the specification for SDC1 is separately described for the xx' , yy' and u planes. BDC3 is a high rate drift chamber which was used in the beam line spectrometer in the K6 beam line at KEK, and it can be operated at as high counting rate as 1 MHz per wire. BDC3 is considered to be placed between TR1 and TR2. SDC1 consists of xx' , yy' and u planes. It has a large area as $120 \times 90 \text{ cm}^2$. It will be mounted at the exit of the ALADiN magnet

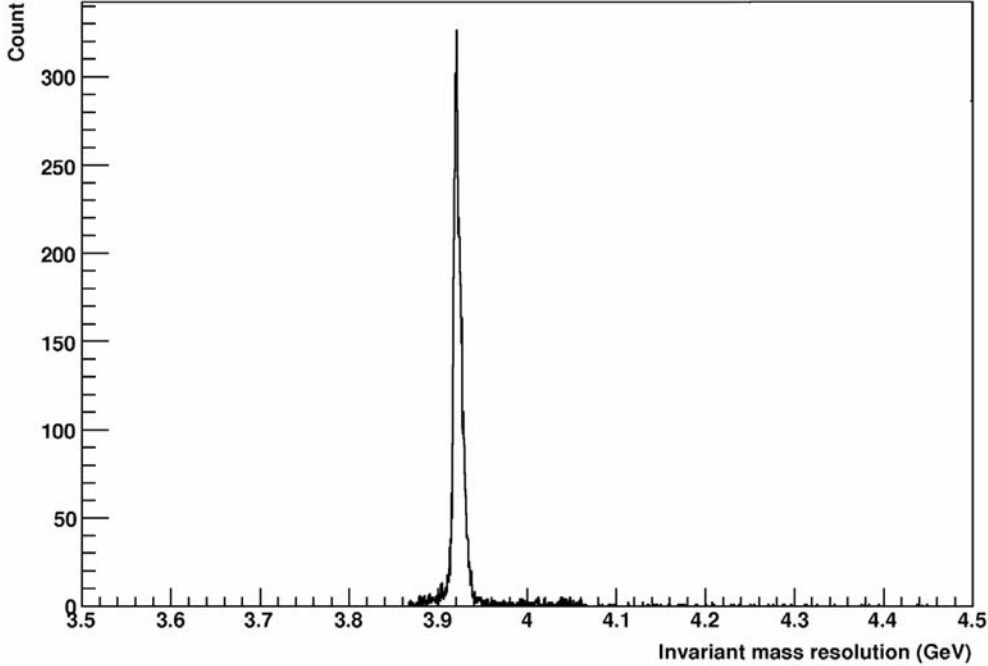


Figure 11: An invariant mass spectrum of ${}^4_{\Lambda}\text{H}$ reconstructed by the proposed setup with the designed TOF+ but without drift chambers and a K^+ detector.

Table 3: Specification of drift chambers which are considered for the Phase 0 experiment.

	Effective area [cm×cm]	drift length [mm]	Planes	Resolution (RMS) [mm]	Channels
BDC3	24(w)×15(h)	2.5	xx'uu'vv'	0.3	288
SDC1XY	120(w)×90(h)	4.5	xx'yy'	0.3	448
SDC1U	120(w)×90(h)	9.0	u	0.4	80

to measure all charged particles going through the ALADiN magnet. Since it can not be operated at high rate, high voltage for several wires around the beam track will not be applied. For the readout electronics, modules with ASD chips from Osaka University and Osaka Electro-Communication University will be used. Logic signals from these modules will be processed with 2.5 ns time granularity by using VUPROM which is developed for the tracking trigger.

3 Progress on transport calculations as event generator of Monte Carlo simulations

In the letter from G-PAC 33, there are discussions on the UrQMD calculations [15] which we used as an event generator for Monte Carlo simulations of the Phase 0 experiment. The letter emphasizes that the use of UrQMD is not appropriate, and the use of other transport calculations such as IQMD and HSD was proposed. All of us understand that the UrQMD calculations have less physics involved than the IQMD and HSD, and the use of UrQMD

may not be proper at 2 A GeV. However, hereby, we would like to clarify on our Monte Carlo simulations presented in the proposal [14]. Since all of UrQMD, IQMD and HSD solve transport equations on the nucleon bases and since they never form any nuclear and hypernuclear fragments by themselves, fragments have to be formed by a second step with having several cut conditions on the kinematics parameters of produced particles, such as by gating on momenta, rapidities and positions of all the particles in the particle list of the result of the calculations for each event. In the Event generator of the HypHI Monte Carlo simulations, nuclear and hypernuclear fragments are produced with the particle list of the UrQMD calculations by gating on the rapidity and the laboratory angle of nucleons and Λ -hyperons at the target and projectile rapidity regions. This process might not be appropriate, however, it should be clearly noted that the formation mechanism of hypernuclei with a heavy ion collision has not been yet known because of lack of experimental data, and it is what the HypHI collaboration aims to investigate. The question to the hypernuclear formation mechanism can not be clearly answered now but can be answered later with the experimental results of the HypHI Phase 0 experiment. In the Monte Carlo simulations presented in the proposal of the HypHI Phase experiment to G-PAC 33 [14], a hypernuclear production cross section was not taken from the UrQMD calculations, however, we used a cross section deduced from the measured cross section for ${}^4_{\Lambda}\text{H}$ in the experiment at JINR in 1988 by scaling with a Λ production cross section of proton-proton collisions. Therefore, the UrQMD calculations do not affect the production rate of hypernuclei. The UrQMD calculations affect only the kinematics of produced hypernuclei, which is affected by the kinematics of Λ -hyperons at forward angles. In the Monte Carlo simulations presented in the proposal [14], kaons are not used for event reconstructions, therefore, the UrQMD calculations on kaons do not affect the result of the simulations. Most crucial part in the UrQMD calculations for the Monte Carlo simulations presented in the proposal [14] is the distribution of pions from the target because the background events in the HypHI Phase 0 experiment are dominated by pion production reactions. The cross section for the pion production reaction is deduced by scaling the nucleon-nucleon collision data. Another dominant background components are due to a free- Λ decay. The amount of free- Λ hyperons in the simulations is deduced by assuming a coalescence probability of Λ in projectile and target fragments as 1 %, therefore, the background calculation also do not employ a cross section from the UrQMD calculations.

Nevertheless, in order to understand more on transport calculations and the event generator of the HypHI Monte Carlo simulations, IQMD calculations have been performed for a ${}^6\text{Li}$ projectile at 2 A GeV on a ${}^{12}\text{C}$ target, with the help of Y. Leifels of the FOPI collaboration. Results of IQMD calculations are compared to the ones of UrQMD calculations, the part of which will be discussed in the next sub-section. In addition to the IQMD calculations, another transport calculation with a formation of nuclear and hypernuclear fragments has been performed by the group of Professor Lenske in Giessen University (Giessen Boltzmann-Uehling-Uhlenbeck project GiBUU), and the result of the calculations will also be presented later in this report. In addition to those transport calculations, production of hypernuclei in multi-fragmentation of nuclear spectator matter is recently discussed by A.S. Botvina and J. Pochodzalla [16].

3.1 Comparison between UrQMD and IQMD

IQMD calculations were performed at a similar condition of the UrQMD calculations used in the HypHI Monte Carlo simulations presented in the proposal [14], a ${}^6\text{Li}$ beam at 2 A GeV on a ${}^{12}\text{C}$ target with an impact parameter distribution to cover the whole collision. Results of the IQMD and UrQMD calculations are presented in the nucleon-nucleon center-of-mass frame. We have looked into the rapidity distributions of Λ and π^- which af-

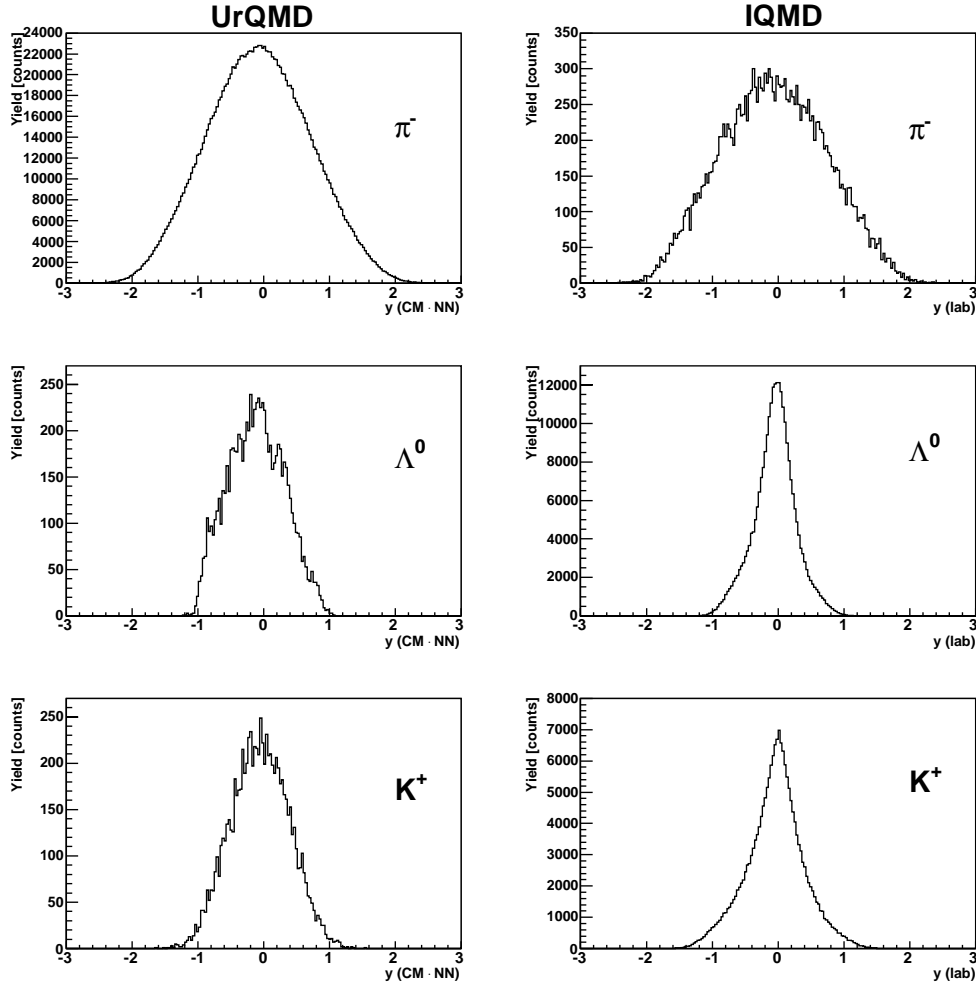


Figure 12: Rapidity distributions obtained from UrQMD (left) and IQMD (right) calculations for π^- (top), Λ (middle) and K^+ (bottom). Distributions for π^- are similar in the both calculations, while difference on Λ and K^+ is observed. See the text for details.

fect the kinematics of produced hypernuclei and the level of background events, respectively. In addition, the rapidity distribution of K^+ is investigated because the HypHI collaboration is currently designing a detector for K^+ on the side wall in the cavity of the ALADiN magnet. Figure 12 shows rapidity distributions of π^- (top), Λ (middle) and K^+ (bottom) obtained from the UrQMD (left) and IQMD (right) calculations. The UrQMD calculations were performed with all collisions, while the IQMD calculations were made with kaon productions. In the figure, a similarity of rapidity distributions of π^- in the both calculations is shown, which indicates that the background induced by π^- in the simulations presented in the proposal is not affected by the choice of either UrQMD or IQMD. It is observed in the figure that the rapidity distribution of Λ is significantly different. Figure 13 taken from ref. [17] shows a comparison of the differential yield distributions for K^0 and Λ^0 among UrQMD and IQMD calculations with medium modifications (w. pot.) and without it (no pot.). Calculations are also compared to the experimental data (filled circles). For the rapidity distribution of Λ^0 , it is clearly observed in the figure that the UrQMD calculation reproduced the experimental data, while none of IQMD calculations can not reproduce the experimental data. The width of the rapidity distribution of Λ affects on the kinematics of produced hypernuclear momenta in the HypHI Monte Carlo simulations. For the rapidity

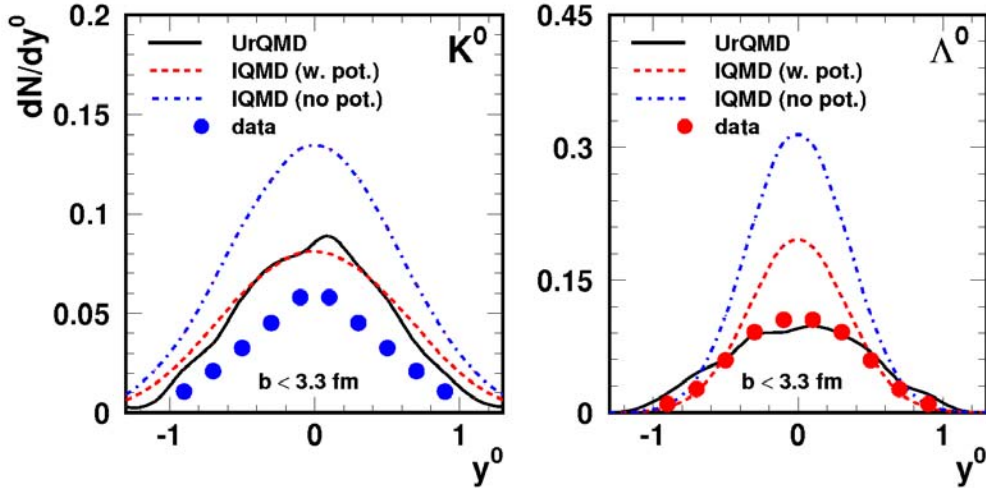


Figure 13: Comparison of the differential yield distributions for K^0 and Λ^0 among UrQMD and IQMD calculations with medium modifications (w. pot.) and without it (no pot.). Calculations are also compared to the experimental data (filled circles). The figure is taken from ref. [17].

distribution for kaons, it is shown in the figure that the choice of either IQMD or UrQMD as an event generator would not affect the design study of the K^+ detector for the Phase 0 experiment because their distributions are similar. It should be noted that the kaon distribution do not affect the result of the Monte Carlo simulation presented in the proposal [14] because we did not demand to detect kaons for those simulations. Even though the rapidity distributions for Λ in the UrQMD and IQMD calculations are different, this difference is not crucial to optimize the experimental setup, therefore, the design of the experimental setup presented in the proposal [14] do not depend on the choice of either UrQMD or IQMD.

It should be noted that momenta of particles in the event generator to Monte Carlo simulations are one of the most crucial information. One has to carefully check if the momentum is conserved in an event because an event generator without conservation of kinematics could drive the design study of the detector system to a wrong direction. Especially for the trigger design, the correlation of particles in the event generator is crucial. Therefore, in order to investigate the goodness of UrQMD and IQMD as an event generator for the HypHI Monte Carlo simulations, the conservation of momenta of all the particles in an event is checked for the both UrQMD and IQMD calculations. Figure 14 shows a total sum of momentum components, x - (top) y - (middle) and z - (bottom) directions, for UrQMD (left) and IQMD (right). It is clearly shown in the figure that momenta are conserved in the UrQMD calculations (perfectly for x and y and almost perfect for z). However, the IQMD calculations do not conserve the momentum for the most of the events.

We would like to emphasize that we do not discuss on which QMD calculation is better. We understand that the choice of IQMD to study the experimental results could be more appropriate than UrQMD at an energy of 2 A GeV. However, there should be rooms for improvements for the theoretical models for heavy ion collisions, and there is information missing especially on the hypernuclear production with heavy ion beams. It can be investigated much more in details when the experimental data of the HypHI project is available. With experimental data, a comparison among the different theoretical models is more fruit-

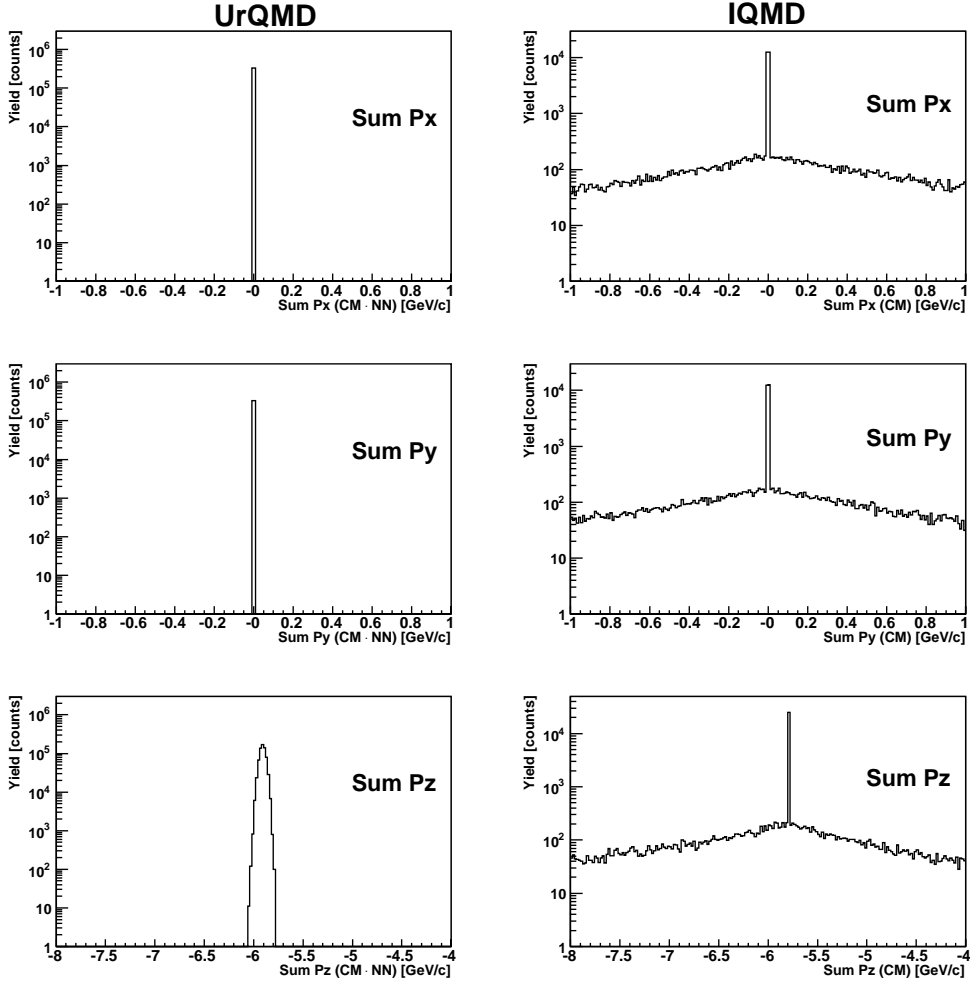


Figure 14: Rapidity distributions of the sum of momenta of all produced particles in one event for UrQMD (left) and IQMD (right) calculations in the x - (top), y - (middle) and z - (bottom) components. It is clearly observed that the momentum is not conserved in many cases in the IQMD calculations.

ful. Therefore, we would insist that there should be no reason to stop the HypHI Phase 0 experiment by the issue of the event generator.

In addition to the UrQMD and IQMD calculations, we also investigate another transport calculations recently performed by the group of Professor Lenske in the Giessen University as a part of the Giessen Boltzmann-Uehling-Uhlenbeck project (GiBUU) [18], which will be discussed in the next sub-section.

3.2 New calculations by the Giessen Boltzmann-Uehling-Uhlenbeck project (GiBUU)

The Giessen Boltzmann-Uehling-Uhlenbeck project (GiBUU) [18] aims to provide a unified transport framework for electron, photon, neutrino, and hadron (especially pion) induced reactions on nuclei, and for heavy-ion collisions. For those reactions, the flow of particles is modeled within a Boltzmann-Uehling-Uhlenbeck (BUU) framework. The relevant degrees of freedom are mesons and baryons which propagate in mean fields and scatter

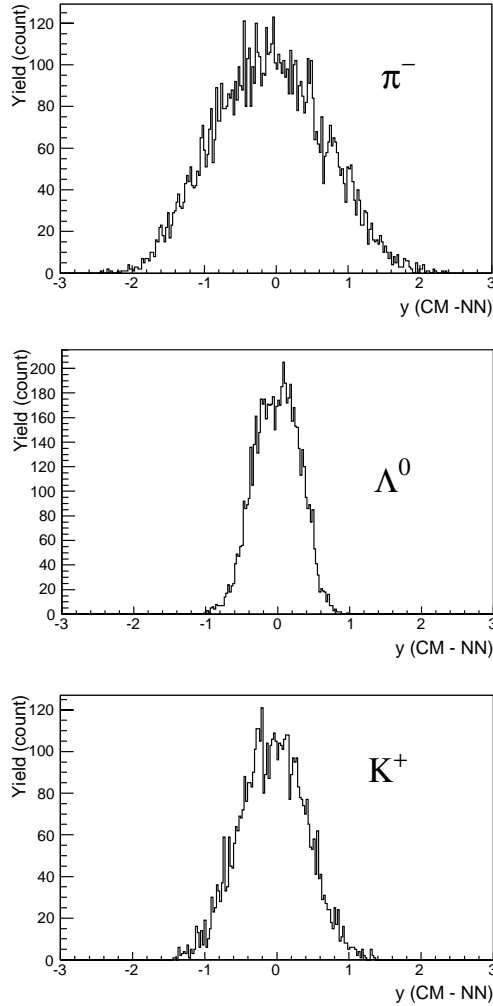


Figure 15: Rapidity distributions by the GiBUU calculations for π^- (top), Λ (middle) and K^+ (bottom).

according to cross sections which are tuned to the energy range of 10 MeV to more than 10 GeV. Calculations for production of hypernuclei with heavy ion beams have been initiated by T. Gaitanos, H. Lenske and U. Mosel of Giessen University, and very recently a collaboration between the GiBUU project and the HypHI project has been started. The GiBUU team is currently providing the results of calculations of a reaction induced by ${}^6\text{Li}$ beams at 2 A GeV on a ${}^{12}\text{C}$ target for the HypHI Phase 0 experiment. In the calculations, nuclear and hypernuclear fragments are formed by a simple coalescence in the simple phase-space. The excitation of formed fragments by coalescence can also be considered, which could induce decays of the fragments with a probability defined as a ratio of the binding energy of the fragments to the total energy with taking a finite lifetimes of the fragments into account. In the GiBUU calculations, energies, momenta, isospins and strangeness are conserved.

Figure 15 shows rapidity distributions for π^- (top), Λ (middle) and K^+ (bottom) obtained from the GiBUU calculations. The distribution of π^- is similar to those in the UrQMD and IQMD calculations. The distribution of Λ is narrower than that in the UrQMD calculations and is wider than IQMD. The width of the rapidity distribution of K^+ by the GiBUU calculation is similar to UrQMD. Since the GiBUU calculations can also form fragments and hypernuclear fragments by using the result of its transport calculations, it is interesting

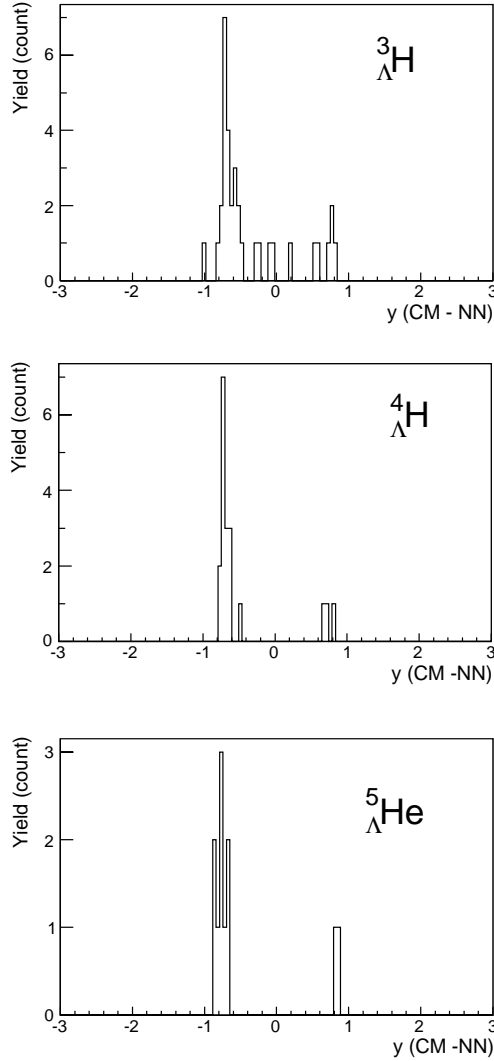


Figure 16: Rapidity distributions by the GiBUU calculations for ${}^3_{\Lambda}\text{H}$ (top), ${}^4_{\Lambda}\text{H}$ (middle) and ${}^5_{\Lambda}\text{He}$ (bottom).

to have a look at the rapidity distribution for hypernuclei of interest, namely ${}^3_{\Lambda}\text{H}$, ${}^4_{\Lambda}\text{H}$ and ${}^5_{\Lambda}\text{He}$. Figure 16 shows the rapidity distribution by the GiBUU calculations with the current available statistics for ${}^3_{\Lambda}\text{H}$ (top), ${}^4_{\Lambda}\text{H}$ (middle) and ${}^5_{\Lambda}\text{He}$ (bottom). Even though the statistics is not enough for the detailed investigation, one can observe a trend of the distributions. For lighter hypernuclei such as ${}^3_{\Lambda}\text{H}$, the rapidity is widely distributed including the mid rapidity region. However, for heavier hypernuclei such as ${}^4_{\Lambda}\text{H}$ and ${}^5_{\Lambda}\text{He}$, the distribution is dominated at the target and projectile rapidity regions. In the proposal [14], the result of Monte Carlo simulations for the ${}^4_{\Lambda}\text{H}$ was presented with the UrQMD calculations as an event generator. As discussed in the previous sub-sections, the production of hypernuclei was performed by cuts on the rapidity and the angle of the particles at the target and projectile rapidity region. Since the produced ${}^4_{\Lambda}\text{H}$ hypernuclei in the GiBUU calculations are dominated at the projectile and target rapidity regions and since the Λ rapidity distribution in the GiBUU calculations is similar to the one with the UrQMD calculations, it is expected that the result of Monte Carlo simulations with the GiBUU calculations as an event generator could be similar to the one presented in the proposal [14]. We are currently increasing the statistics for the GiBUU calculations, and the result of Monte Carlo simulations with the GiBUU

calculations will be presented in the meeting of G-PAC 34.

4 Conclusion and request

For a further step toward the Phase 0 experiment, a number of experimental developments and investigations for detectors have been performed. Since the scintillating fiber detectors are the most essential parts of the Phase 0 setup for tracking and triggers, two prototypes of scintillating fiber detectors with different versions of HAMAMATSU photomultipliers, H7260K and H7260KS, were tested with cosmic-rays, β -rays, lasers, a ^{12}C beam at 2.4 GeV and a cocktail beam at 3.3 Tm. The results of the test measurements reveals the capability of the proposed fiber detector in the Phase 0 experiment for the energy measurements and tracking. With these investigations, the design of scintillating fiber detectors was finalized as shown in Table 2. Prototype modules of the newly developed VME logic modules VUPROM were also tested during the beam-time in cave A with the ^{12}C primary beams and the cocktail beam. In the test experiment, the most important part of the tracking trigger, the on-line clustering on board, was performed, and the feasibility of the on-line-clustering at FPGA was shown. It was also shown in the analysis that it doesn't take long time to perform on-line-clustering on boards, therefore, the total trigger formation time for the tracking trigger with the proposal ways with further multiple coincidences could not take longer than 500 ns. It has already appeared that the tracking trigger should meet no problem in the Phase 0 experiment.

In addition to the investigations on the fiber detector and the tracking trigger, the design study of a TOF wall for positively charged particles, TOF+, meets the final stage with the Monte Carlo simulations. The Monte Carlo simulations for the study of TOF+ also reveals that the data analysis with a real field map for the ALADiN magnet can be performed by the algorithm of the analysis with a well-like distribution of the magnetic field, which was presented in the proposal. DFG has granted for the development of TOF+ with an investment budget of 180 k Euro and one postdoc position for two years.

The HypHI collaboration also succeeded to get two drift chambers from KEK in order to increase the redundancy of tracking. The drift chambers are currently being tested in KEK, and they will be delivered from KEK to GSI in summer 2007 with associated electronics modules from Osaka University and Osaka Electro-Communication University. The design study of a K^+ detector on the side wall in the cavity of the ALADiN magnet is in progress, and the design study will be finished in a couple of months.

In order to answer to the criticism in the letter from G-PAC 33 for the event generator of the HypHI Monte Carlo simulations, investigations on UrQMD and IQMD calculations were performed. The similarity of the pion distributions suggest that the background level in the Monte Carlo simulations is not affected by the choice of either UrQMD or IQMD. The rapidity distribution of the Λ -hyperon by the UrQMD calculations can reproduce experimental data without modifications, however, any of IQMD calculations can not reproduce the experimental Λ distribution. It was also shown that the momentum is conserved in the UrQMD calculations, while it is not conserved in the IQMD calculations. The letter from the G-PAC 33 criticized the use of UrQMD for estimating the production rate. As discussed in the previous sections, we did not use the UrQMD calculations to estimate the cross sections. The cross sections are estimated by using the experimental data, therefore, the choice of either UrQMD or IQMD do not affect the production rate. The results of the UrQMD calculations are used only for kinematics for the hypernuclear event.

Table 4: Preliminary rate estimate for reconstructed hypernuclei per week in the Phase 0 experiment with the current setup.

	Expected cross section [μb]	Reconstructed events /week
${}^3_{\Lambda}\text{H}$	0.1	2.8×10^3
${}^4_{\Lambda}\text{H}$	0.1	2.6×10^3
${}^5_{\Lambda}\text{He}$	0.5	6.5×10^3

It must be noted here that we are not discussing on which QMD calculation is better. We have already understood that the IQMD model contains more physics and could be proper at 2 A GeV to compare to the experimental data. However, it should be also noted that one can not come to the conclusion for this discussion because of lack of experimental data for the hypernuclear production with heavy ion beams. It should be noted that the HypHI collaboration will contribute experimentally to this investigation. This discussion can be opened again when the HypHI data is available. Therefore, the HypHI collaboration do not see any reason that the GSI PAC is stopping the Phase 0 experiment by the issue of the event generator.

Recently, a collaboration between the GiBUU project and the HypHI project has been started, and detail studies on the Monte Carlo simulations with the GiBUU calculations as an event generator is in progress. The part of results with increased statistics will be presented in the meeting of G-PAC 34.

According to all the investigations discussed in this report, the result of the Monte Carlo simulations and rate estimate presented in the proposal of the Phase 0 experiment remains unchanged. The estimation for the Phase 0 experiment is again shown in Table 4. Therefore, we still request the same amount of beam times for the Phase 0 experiment, and the request is repeated here.

Since the hypernuclear production cross section and the Λ coalescence factor have not yet been known, we would like to be in the safe side. We would like to accumulate at least 4000 reconstructed events for the case of ${}^4_{\Lambda}\text{H}$ assuming 0.1μ barn production cross section. Therefore, we would like to request 11 days of beams on target (33 shifts). With this statistics, the polarization measurement of hypernuclei can also be achieved, and the significance of the ${}^4_{\Lambda}\text{H}$ invariant mass peak is expected to be approximately 48σ with the current cut condition. If the cross section is one order of magnitude smaller, we can still reconstruct 400 ${}^4_{\Lambda}\text{H}$ events with a 5 % statistical error. Since, we are still improving the experimental setup and the analysis procedure, it is expected that the experiment is feasible with this lower statistics. Therefore, 11 days of beams on the target is strongly requested. We would like to ask one day (3 shifts) for the beam adjustment, and three days (9 shifts) for the calibration of the detector systems with the beams. Therefore, **we would like to ask 15 days (45 shifts) with ${}^6\text{Li}$ beams in cave C.** We request a beam of ${}^6\text{Li}$ at 2 A GeV with an intensity of 1.2×10^8 per spill with periods of acceleration and extraction being respectively 2 and 10 seconds, and the beam spot size at our target in cave C is 1 cm in σ of Gaussian distribution.

In addition to this beam time request, we would like to ask an opportunity to use parasitic beams (most probably to the cancer therapy) for testing detectors in any caves available at that time.

The HypHI collaboration would like to thank to the GSI accelerator department, the GSI safety department, D. Schardt of the Bio-Physics department at GSI, H. Iwase of KEK and R. Simon of KP1 at GSI for their kind supports for the test experiment in March 2007. The HypHI collaboration would also like to thank to the Detector Laboratory, the EE department at GSI and I. Kojouharov of KP2/GSI for their support on the development of detectors and electronics modules. The HypHI collaboration would like to present a gratitude to Y. Leifels of GSI, T. Gaitanos, H. Lenske and U. Mosel of Giessen University for discussions on the transport calculations.

The HypHI project is granted by the Helmholtz Association and GSI as Helmholtz-University Young Investigators Group VH-NG-239.

References

- [1] <http://www.lnf.infn.it/esperimenti/finuda/finuda.html>
- [2] <http://lambda.phys.tohoku.ac.jp/~hks/>
- [3] <http://wwwa1.kph.uni-mainz.de/A1/KAOS/>
- [4] <http://j-parc.jp/>
- [5] <http://lambda.phys.tohoku.ac.jp/~tamura/hyperball/>
- [6] http://www.gsi.de/forschung/kp/kp3/index_e.html
- [7] Letter Of Intent of “Hypernuclei with Stable Heavy Ion Beam and RI-beam Induced Reactions at GSI (HypHI)”. LOI can be obtained at http://www.gsi.de/forschung/kp/kp2/experiments/HYPERNuclei/index_e.html
- [8] A.K. Kerman and M.S. Weiss, Phys. Rev. **C8** (1973) 408.
- [9] A.U. Abdurakhimov, *et al.*, Nuovo Cimento **A102** (1989) 645.
- [10] S. Avramenko, *et al.*, Nucl. Phys. **A547** (1992) 95c.
- [11] M. Wakai, H. Bando and M. Sano, Phys. Rev. **C38** (1988) 748.
- [12] M. Sano and M. Wakai, Prog. of Theor. Phys. Suppl. **117** (1994) 99.
- [13] T.A. Armstrong *et al.*, Phys. Rev. **C70** (2004) 024902.
- [14] Proposal of the HypHI Phase 0 experiment submitted to the G-PAC 33 in October 2006.
- [15] <http://www.th.physik.uni-frankfurt.de/~urqmd/>
- [16] A.S. Botvina and J. Pochodzalla, to be published.
- [17] M. Merschmeyer, Ph.D. thesis, the Ruperto-Carola University of Heidelberg, Germany, 2004.
- [18] Private communications to T. Gaitanos, H. Lenske and U. Mosel. <http://tp8.physik.uni-giessen.de:8080/GiBUU/>